



TITLE:

# Response Function of a 1-inch Diameter by 6-inch Long $^3\text{He}$ Proportional Counter to Neutrons

AUTHOR(S):

NISHINO, Seiji; NAKAMURA, Takashi; HYODO, Tomonori

---

CITATION:

NISHINO, Seiji ...[et al]. Response Function of a 1-inch Diameter by 6-inch Long  $^3\text{He}$  Proportional Counter to Neutrons. Memoirs of the Faculty of Engineering, Kyoto University 1973, 35(3): 309-329

ISSUE DATE:

1973-09-29

URL:

<http://hdl.handle.net/2433/280923>

RIGHT:

# Response Function of a 1-inch Diameter by 6-inch Long $^3\text{He}$ Proportional Counter to Neutrons

By

Seiji NISHINO\*, Takashi NAKAMURA\* and Tomonori HYODO\*

(Received March 31, 1973)

## Abstract

The response of a 1-inch diameter by 6-inch long  $^3\text{He}$  proportional counter, of which the gas filling is 4 atm  $^3\text{He}$  and 2 atm krypton, to axially incident neutrons has been studied and expressed as a 50 by 50 matrix for an energy range from zero to 5 MeV. Applications of the matrix were examined for the purpose of obtaining response-corrected spectra of neutrons transmitted through a matter.

## 1. Introduction

Recently a  $^3\text{He}$ -filled proportional counter has been used as a neutron spectrometer, since it has some advantages for this purpose.<sup>1)-4)</sup> The  $^3\text{He}(n, p)\text{T}$  reaction is suitable for neutron spectroscopy, because its reaction cross section is reasonably large and varies slowly with energy, and the  $Q$ -value of the reaction ( $Q=764$  keV) is large enough to separate the pulses due to neutrons from gamma-ray pulses.

There is ambiguity in the pulse height distribution originating from monoenergetic neutrons, excluding the intrinsic Gaussian distribution of pulse-height. The ambiguity is caused by elastic scattering of neutrons by counter gas and wall- and end-effect.

The pulse-height distribution obtained by a  $^3\text{He}$  counter for monoenergetic neutrons is mainly composed of three parts:  $^3\text{He}(n, p)\text{T}$  reaction peak, the location of whose top is at the sum of energy  $Q$  and incident neutron energy  $E_n$ ,  $^3\text{He}$ -recoil distribution from 0 to  $4 E_n$ , and wall- and end- effect distribution from 0 to  $E_n + Q$ . Contribution of the  $^3\text{He}(n, d)\text{D}$  reaction is negligibly small, because of a high threshold energy (4.3 MeV) and a small cross section.

---

\* Department of Nuclear Engineering

In the practical application, a  $^3\text{He}$  counter usually indicates a large thermal neutron peak in the pulse height distribution. This is because there is a large amount of background neutrons in a room and the thermal neutron cross section of  $^3\text{He}(n, p)\text{T}$  reaction is very large (5,460 barns).

Some efforts have been made to reduce the complex pulse-height distribution to the neutron spectrum. The risetime discrimination was applied to distinguish between pulses from the  $^3\text{He}(n, p)\text{T}$  and  $^3\text{He}(n, n)^3\text{He}$  reactions.<sup>(5)</sup> A wall-less counter was constructed to eliminate the wall effect.<sup>(6)</sup> The pulse-height distribution obtained by a  $^3\text{He}$  counter was mathematically converted to a neutron energy spectrum by using the response function matrix.<sup>(3),4)</sup>

In our study, the mathematical conversion method was chosen, because a wall-less counter could not be obtained and the rise-time discrimination decreased the counter efficiency. No response function matrix for a 1-inch diameter by 6-inch long  $^3\text{He}$  proportional counter, of which the gas filling is 4 atm  $^3\text{He}$  and 2 atm krypton, has been reported. The response function of a cylindrical  $^3\text{He}$ -filled proportional counter must be obtained experimentally or by the Monte Carlo simulation, because it cannot be expressed by any exact analytic formula. The counter responses were measured to various monoenergetic neutrons, and the response function matrices for the neutron energy which range from zero to 5 MeV were calculated from interpolation of the measured responses with FACOM 230-60 computer of Kyoto University. In this paper, a table of the response function matrix composed of 50 rows by 50 columns is presented.

## 2. Experimental

A block diagram of the measuring system is shown in Fig. 1. The  $^3\text{He}$  counter used is 1-inch in diameter and 6-inch in active length, filled with  $^3\text{He}$  gas to 4 atm and

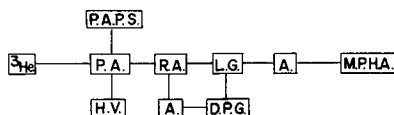


Fig. 1. Block diagram of the measuring system.

- $^3\text{He}$  :  $^3\text{He}$  Proportional counter
- P.A. : Pre-amplifier (ORTEC Model 109 PC)
- P.A.P.S. : Pre-amplifier power supply
- H.V. : High voltage power supply
- R.A. : Research amplifier (ORTEC Model 450)
- A. : Amplifier (ORTEC Model 485)
- L.G. : Linear gate and slow coincidence (ORTEC Model 409)
- D.P.G. : Delayed pulse generator<sup>(7)</sup>
- M.P.H.A.: Multichannel pulse height analyzer

krypton gas to 2 atm (Texas Nuclear Co. Model 9341), and is covered with 2.5 mm-thick cadmium in order to reduce the thermal neutron back-ground.

Since the rise-time of pulses from a gas-filled proportional counter is not unique and longer than the clipping time of an ordinary linear amplifier, a special sampling method was applied to eliminate the effect of the spread of rise-time and to improve the energy resolution. In the measuring system, the output pulses from the pre-amplifier are fed to the research amplifier, where pulse shaping (differentiation and integration) and amplifying are performed. The pulse height is sampled at about 10  $\mu$ sec after the start of the output pulse from the amplifier, by means of the delayed pulse generator<sup>7)</sup> and the linear gate and slow coincidence. These pulses are amplified and fed to a multi-channel pulse-height analyzer. The energy resolution of this system is about 7% in F.W.H.M. (=about 50 keV) for thermal neutrons, while it is

Table 1. List of neutron energy used in this experiment.

Reactions	Acceleration Voltage (MV)	Emergent Angle* (degree)	Neutron Energy (MeV)	Accelerators
$T(p, n)^3\text{He}$	1.5	90	0.147	Van de Graaf
	1.8	90	0.272	
	1.26	0	0.348	
	1.35	0	0.455	
	1.5	30	0.525	
	1.52	0	0.642	
	2.70	90	0.754	
	1.73	0	0.868	
	1.8	0	0.890	
	1.89	0	1.040	
	2.09	0	1.243	
	2.33	0	1.497	
	2.5	0	1.668	
	2.62	0	1.795	
	2.8	0	1.873	
2.93	0	2.103		
3.0	0	2.178		
$D(d, n)^3\text{He}$	0.2	120	2.276	Cockcroft-Walton
		90	2.485	
		60	2.718	
		30	2.923	
$T(p, n)^3\text{He}$	4.0	0	3.190	Tandem Van de Graaf
	4.5	30	3.332	
	4.5	0	3.694	
	5.0	0	4.197	
	5.3	0	4.499	
	5.5	0	4.700	
6.0	0	5.202		

\* This angle indicates the polar angle between axes of accelerated particle beam and detector.

about 15% or more with the conventional system.

For the purpose of counter response measurement, various monoenergetic neutrons were produced from the  $T(p, n)^3\text{He}$  and  $D(d, n)^3\text{He}$  reactions, using a Van de Graaf accelerator and a Cockcroft Walton accelerator at the Department of Nuclear Engineering, Kyoto University, and a Tandem Van de Graaf accelerator at the Department of Physics, Kyoto University. The D-target and T-target used in these experiments were solid targets that deuterium and tritium were adhered to zirconium which had been evaporated onto copper in vacuum. The energy of the produced neutrons was calculated by considering the energy losses of protons and deuterons. The responses were obtained experimentally for 28 mono-energetic neutrons from 0.15 MeV to 5.20 MeV, which are listed in Table 1. The measured responses to 0.89 MeV, 2.48 MeV and 3.69 MeV neutrons are shown in Fig. 2, as examples.

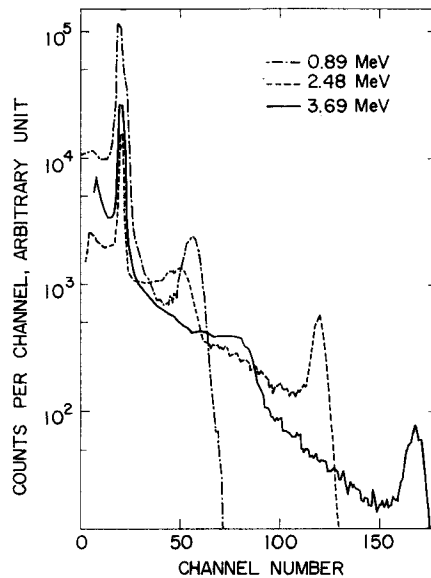


Fig. 2. Measured counter responses for monoenergetic neutrons.

### 3. The Response Function Matrix

In this paper, two response function matrices are presented. One is the response function matrix for the simple method,<sup>8),9)</sup> the other is that for the inverse matrix method, etc.<sup>3),4),9)</sup> Both of them were interpolated from the measured counter responses and normalized to the parallel beam of neutrons of a unit flux which was incident axially to the counter.

1) Modification of Measured Pulse-Height Distribution

The measured pulse-height distribution was modified to a response function suitable for calculation of the response function matrix by the following procedure.

a) The Fast Neutron Peak

The following two assumptions were made. For the response function of the inverse matrix method etc., the  $^3\text{He}(n, p)\text{T}$  full energy peak for fast neutrons is of a Gaussian distribution, of which the width is proportional to the square root of the sum of  $E_n$  and  $Q$ , and the total counts are equal to those of the measured fast neutron peak when the mono-energetic neutrons of an unit flux are incident axially to the counter. The pulse-height at the maximum of the Gaussian distribution is proportional to  $E_n + Q$ .

For the response function of the simple method, the fast neutron peak is not Gaussian, but is rectangular, of which the width is equal to that of the energy group ( $\Delta E = 0.1 \text{ MeV}$ ), and the channel of the pulse-height corresponds to  $E_n + Q$ .

b) The  $^3\text{He}$ -Recoil Distribution and the Wall- and End-Effect Distribution

We assumed that the pulse-height distributions due to the  $^3\text{He}(n, n)^3\text{He}$  reaction and the wall- and end-effect for fast neutrons are of the same shape as those of the measured response.

c) Estimation and Reduction of Thermal Neutron Contribution

The full energy peak and the wall- and end-effect caused by thermal neutron backgrounds were removed from the measured pulse-height distribution by the procedure shown in Fig. 3.

The response function for the thermal neutrons which are incident parallel to the counter axis was calculated by the method described by Shalev et al.<sup>10)</sup> Writing the distribution function for the pulse-height  $E'$  as  $F(E')$ , the following relationship is obtained for the wall- and end-effect and for the full energy peak due to thermal neutrons, respectively. For the full energy peak, it can be expressed as

$$F_p(E') = 1 - \frac{1}{D'} \{ (S_p)_{\text{mixt.}} + (S_t)_{\text{mixt.}} \} \quad (1)$$

when  $D'$  is defined as

$$\frac{1}{D'} = \frac{1}{D} + \frac{1}{2L} \quad (2)$$

where  $D$  is the diameter of the counter,  $L$  the active length of the counter, and  $(S_p)_{\text{mixt.}}$  and  $(S_t)_{\text{mixt.}}$  the ranges of 573 keV protons and 191 keV tritons in the gas-filling of the counter (4 atm  $^3\text{He}$  and 2 atm Kr), respectively. For the wall- and end-effect, it can be written as

$$F_W(E') = \frac{1}{D'} \left[ \left\{ \frac{(S_p)_{\text{m1xt.}}}{(S_p)_{\text{Kr}}} \right\} / \left( \frac{dE}{dx} \right)_p + \left\{ \frac{(S_t)_{\text{m1xt.}}}{(S_t)_{\text{Kr}}} \right\} / \left( \frac{dE}{dx} \right)_t \right] \quad (3)$$

where  $(S_p)_{\text{Kr}}$  and  $(S_t)_{\text{Kr}}$  are the ranges of 573 keV protons and 191 keV tritons in krypton, respectively, and  $(dE/dx)_p$  and  $(dE/dx)_t$  are the specific ionization of protons and tritons in krypton, respectively. This distribution was smoothed by a Gaussian distribution, with a standard deviation equal to that obtained experimentally with the counter. The calculated response function for the thermal neutrons is shown in Fig. 3A.

Six points at both ends of the calculated thermal neutron peak were fitted to a cubic equation with the least square method, and the total counts of the calculated thermal neutron peak  $C_t$  (the hatched part in Fig. 3A) were easily obtained. The subtraction of this thermal neutron peak from the response function gave the counts in the  $i$ -th channel of the pulse-height analyzer  $W_i$ , which was due to the wall- and end-effect for thermal neutrons, as is shown in Fig. 3A.

At last, six points at both ends of the thermal neutron peak in the measured pulse-height distribution were also fitted to a cubic equation with the least square method, and the total counts of the measured thermal neutron peak  $C_t'$  (the hatched part in Fig. 3B) were obtained. The quantity  $W_i C_t' / C_t$  was subtracted from the pulse-height distribution,  $C_i'(E_n)$ , which had already got rid of the full energy peak due to thermal neutrons from the measured pulse-height distribution, as shown in Fig. 3B. Then

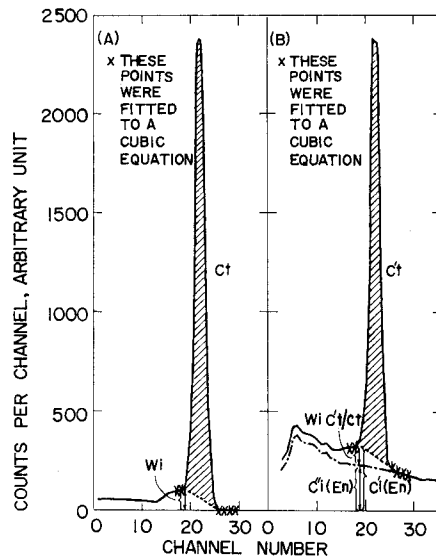


Fig. 3. A schematic illustration of the reduction of thermal neutron contribution.

(A) Calculated response for thermal neutrons.

(B) Thermal neutron peak part of measured counter response.

the resultant pulse-height distribution,  $C_i''(E_n)$ , after removal of thermal neutron peak is described as follows,

$$C_i''(E_n) = C_i'(E_n) - W_i C_t' / C_t \quad (4)$$

We used this distribution,  $C_i''(E_n)$ , as the input data for the determination of the response function matrix.

d) The Counter Efficiency

It was assumed that the pulse-height distribution caused by the wall- and end-effect for fast neutrons extends linearly from zero to  $E_n + Q$ . The pulse-height distribution of the wall- and end-effect was fitted to a linear equation by the least square method, from the channel which corresponds to  $3/4 E_n$  (point a in Fig. 4) to that of the lower end of the fast neutron peak (point b), and it was extrapolated to zero energy as shown in Fig. 4. The total  $^3\text{He}(n, p)\text{T}$  reaction number for fast neutrons  $C_{np}(E_n)$ , which is the sum of the total counts of the fast neutron peak and those of the wall- and end-effect (the hatched part in Fig. 4), was obtained. The efficiency  $\epsilon(E_n)$  of a  $^3\text{He}$  counter for the  $^3\text{He}(n, p)\text{T}$  reaction, when the parallel beam of neutrons is incident axially to the counter and the effect of krypton is neglected, can be written as

$$\epsilon(E_n) = \frac{\pi D^2}{4} \cdot \frac{\sum n p(E_n)}{\sum t(E_n)} [1 - e^{-\Sigma_t(E_n)L}] \quad (5)$$

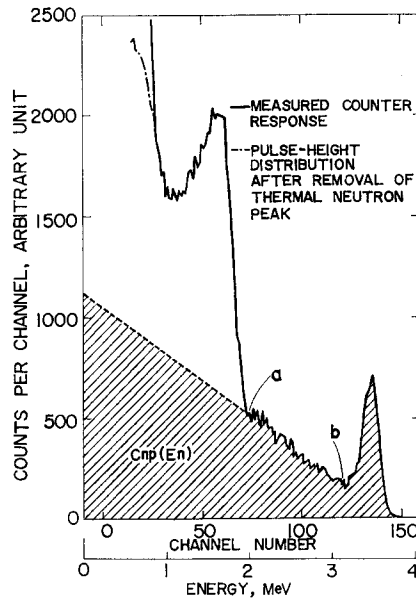


Fig. 4. A schematic illustration of the determination of the total  $^3\text{He}(n, p)\text{T}$  reaction number for fast neutrons  $C_{np}(E_n)$ .



where  $\Sigma_{np}(E_n)$  is the macroscopic  ${}^3\text{He}(n, p)\text{T}$  reaction cross section and  $\Sigma_t(E_n)$  is the total macroscopic cross section. From  $C_{np}(E_n)$  and  $\epsilon(E_n)$ , we can easily obtain the response function  $R'_i(E_n)$  normalized to neutrons of a unit flux which are incident parallel to the counter axis. It is given by

$$R'_i(E_n) = C_{i''}(E_n)\epsilon(E_n)/C_{np}(E_n) \quad (6)$$

## 2) Interpolation of the Response Function Matrix

The pulse-height higher than that corresponding to  $Q$  was adopted as the input data for the response function, since the information to obtain the fast neutron spectrum is sufficient and the effect of gamma-ray back-grounds is almost negligible in this energy range. The response functions calculated from Eq.(6) for 0.89 MeV, 2.48 MeV and 3.69 MeV neutrons are shown in Fig. 5.

From these response functions, two types of response function matrices, as described at the beginning of this chapter, were obtained approximately.<sup>11)</sup> This is because the amount of input data was not enough to give an exact calculation, and the response of a  ${}^3\text{He}$  counter varied slowly with the incident neutron energy. The response function matrix element  $R_{ij}$  was obtained by using an approximate formula,

$$R_{ij} = \frac{G\left(E'_i, E_j - \frac{\Delta E}{2}\right) + 4G(E'_i, E_j) + G\left(E'_i, E_j + \frac{\Delta E}{2}\right)}{6} \cdot \frac{\Delta E}{\Delta E'} \quad (7)$$

where  $G(E'_i, E_j)$  is defined as

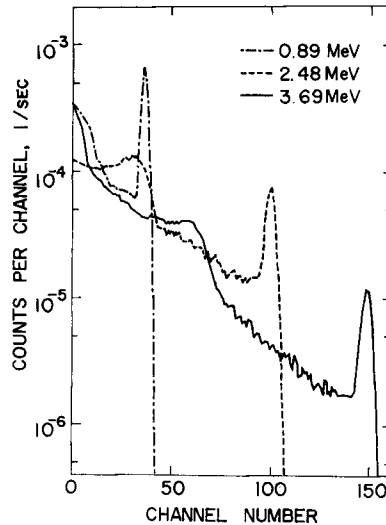


Fig. 5. The response functions calculated from Eq. (6).























$$G(E'_i, E_j) = \int_{E'_i - \frac{\Delta E'}{2}}^{E'_i + \frac{\Delta E'}{2}} R''(E'_i, E_j) dE' \quad (8)$$

where  $R''(E'_i, E_j)$  is the response function of the counter. This is obtained by means of the Lagrange interpolation method from the response function  $R'_i(E_n)$  in Eq.(6).  $E'_i$  and  $E_j$  are the pulse-height of  $i$ -th interval and the neutron energy of  $j$ -th interval, respectively.  $\Delta E'$  and  $\Delta E$  are the intervals of the pulse-height and the energy, respectively.

As a result, the response function matrix, composed of 50 rows by 50 columns, of which the bin width is 0.1 MeV and the energy range from zero to 5 MeV, was obtained. The response function matrix for the simple method and that for the inverse matrix method, etc. are shown in Table 2 and Table 3, respectively.

#### 4. Application of the Response Function Matrix

The response-corrected spectrum ( $\phi$ ) obtained by the inverse matrix method is given by

$$(\phi) = [R_I]^{-1}(P) \quad (9)$$

where ( $P$ ) is the measured pulse-height distribution which has been divided into the pulse-height interval corresponding to the energy interval of 0.1 MeV.  $[R_I]$  is the response function matrix for the inverse matrix method etc.

The response-corrected spectrum ( $\phi'$ ) calculated by the simple method<sup>8),9)</sup> can

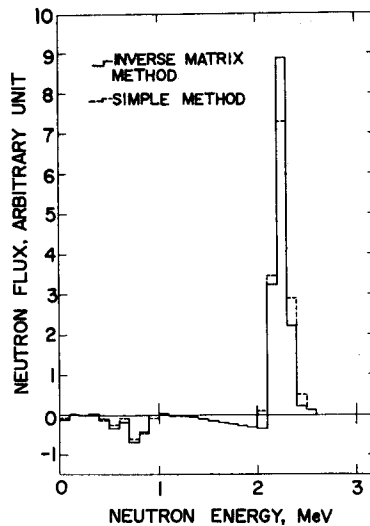


Fig. 6. A response-corrected spectrum for 2.28 MeV monoenergetic neutrons.

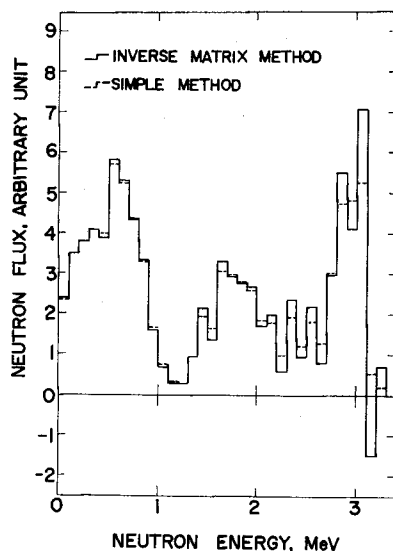


Fig. 7. A response-corrected spectrum of 3 MeV neutrons transmitted through 15 cm-thick iron.

be written as

$$(\phi)=[R_s]^{-1}(P) \quad (10)$$

where  $[R_s]$  is the response function matrix for the simple method.

Fig. 6 shows a typical response-corrected spectrum by means of the above two methods for 2.28 MeV monoenergetic neutrons. A response-corrected spectrum of 3 MeV neutrons transmitted through 15 cm-thick iron is shown in Fig. 7.

### Acknowledgments

The authors wish to thank Messers. H. Hirayama, N. Sawano and Y. Urushidani for their co-operation in the experiment on this study. The authors are grateful to Dr. Y. Furuta and Mr. T. Miura for kindly sending their unpublished data. The authors express their gratitude to Dr. T. Hasegawa for his helpful contribution during the experiment with a Tandem Van de Graaf at the Department of Physics, Kyoto University. The authors are also grateful to Miss K. Todo for her helpful assistance with this paper.

### References

- 1) R. Batchelor, R. Aves, and T. H. R. Skyrme: *Rev. Sci. Instr.* **26**, 1037 (1955).
- 2) R. Batchelor and G. C. Morrison: *Fast Neutron Physics* (ed. J. B. Marion and J. L. Fowler,

- Intersci. Publ. Inc., New York, 1960) Pt. I, 413.
- 3) T. Fuse, T. Miura, A. Yamaji and T. Yoshimura: Nucl. Instr. and Methods, **74**, 322 (1969).
  - 4) T. Iijima, T. Mukaiyama and K. Shirakata: J. Nucl. Sci. and Technol, **8**, 192 (1971).
  - 5) A. Sayres and M. Coppola: Rev. Sci. Instr. **35**, 431 (1964).
  - 6) W. K. Brown: Nucl. Instr. and Methods, **26**, 1 (1964).
  - 7) Y. Furuta: private communication.
  - 8) T. Hyodo: This memoirs, **30**, 187 (1968).
  - 9) S. Nishino, Y. Urushidani, T. Nakamura and T. Hyodo: to be published.
  - 10) S. Shalev, Z. Fishelson and J. M. Cuttler: Nucl. Instr. and Methods, **71**, 292 (1969).
  - 11) T. Hyodo and F. Makino: This memoirs, **24**, 291 (1962).